Electronic Supplementary Information (ESI)

Label-free photoelectrochemical cytosensing via resonance energy transfer using gold nanoparticles-enhanced carbon dots

Shanshan Liu, Huijuan Cao, Zhaoyin Wang, Wenwen Tu* and Zhihui Dai*

Jiangsu Collaborative Innovation Center of Biomedical Functional Materials and Jiangsu Key Laboratory of Biofunctional Materials, School of Chemistry and Materials Science, Nanjing Normal University, Nanjing 210023, P. R. China

*Corresponding author. E-mail: daizhihuii@njnu.edu.cn, wwt@njnu.edu.cn; Fax: +86-25-85891051; Tel: +86-25-85891051

1. Experimental section

1.1 Reagents and materials. Tris (hydroxymethyl) aminomethane (Tris) was purchased from Alfa Aesar China Ltd. N-(3-Dimethylamnopropyl)-N′-ethylcarbodiimide hydrochloride (EDC), chitosan (CS), gold(III)chloride trihydrate, cysteamine (Cys), N-hydroxysuccinimide (NHS), folic acid (FA), bovine serum albumin (BSA) and acridine orange hemi (zinc chloride) salt (AO) were purchased from Sigma-Aldrich. Ascorbic acid (AA) and sodium bicarbonate were obtained from Sinopharm Chemical Reagent Co, Ltd (Shanghai, China). Activated carbon powder (200 mesh) and 3 kDa molecular weight cut-off (MWCO) membranes were purchased from local suppliers. All other reagents were of analytical grade. Tris-HCl buffer saline was used as the washing solution (pH 7.40, 0.01 M) and supporting electrolyte (pH 7.40, 0.1 M). Folic acid molecules were dissolved in Tris-HCl buffer saline (0.01 M, pH 7.40), which exhibited well water-solubility. The

physiological phosphate buffered saline (PBS) solution containing NaCl (136.75 mM), KH_2PO_4 (1.76 mM), Na_2HPO_4 (10.14 mM) and KCl (2.28 mM), was used to wash the cell culture fluid. Ultrapure water obtained from a water purification system (18.25 MΩ·cm, Milli-Q Integral, Millipore Corporation, America) was used in all experiments.

1.2 Apparatus. X-ray diffraction (XRD) patterns were recorded using a D/max 2500 VL/PC diffractometer (Japan) equipped with graphite-monochromatized Cu KR radiation. Ultraviolet-visible (UV-vis) absorption spectra were obtained using a Cary 50 spectrophotometer (Varian, USA). Photoluminescence (PL) spectra were recorded on a Fluoromax-4 spectrofluorometer (Horiba, USA). High-resolution transmission electron microscopy (HRTEM) images were taken on a JEOL-2100F apparatus at an accelerating voltage of 200 kV (JEOL, Japan). The HeLa cells were cultured with a cell incubator (Thermo, USA) and were imaged using an Eclipse Ti-S inverted fluorescence microscope (Nikon, Japan). The PEC measurements were performed with a Zahner photoelectrochemical workstation (Zahner, Germany). All PEC measurement were conducted at room temperature using a conventional three-electrode system with a modified indium tin oxide (ITO) electrode (sheet resistance, 20-25 Ω/square) with a geometrical area of 0.25 cm_2 as the working electrode, a platinum wire as the auxiliary electrode, and a Ag/AgCl electrode as the reference electrode. Electrochemical impedance spectroscopy (EIS) was conducted using an Autolab potentiostat/galvanostat PGSTAT302N (Metrohm, Netherland) with a three-electrode system in KCl solution (0.1 M) containing a $K_3Fe(CN)_6/K_4Fe(CN)_6$ (5.0 mM, 1:1) mixture as the redox probe from 0.1 Hz-100 kHz with a signal amplitude of 10 mV. MTT assays were performed on a microplate reader (Thermo Fisher, USA).

1.3 Synthesis of the C-dots-AuNPs-Cys suspension. C-dots were synthesized according to

a previous report.[S1] the AuNPs-Cys were also synthesized according to a modification of a previously reported procedure.[S2] In particular, the Cys stock solution (0.5 M) was prepared by dissolving 0.03858 g Cys in 1 mL ultrapure water and then stored in the refrigerator at 4 °C. 60 μL Cys stock solution (0.5 M) was injected into 15 mL $HAuCl_4$ (1 mM) under stirring, and then 5 mL $NaBH_4$ solution (8 mM) that had been cooled to 4 °C was added drop-wise. After the mixture turned from yellow to wine red, the unreacted reagents were removed via dialysis for 24 h with 3000 molecular weight dialysis membrane in ultrapure water to obtain AuNPs-Cys colloid suspension (0.1 $mg \cdot mL^{-1}$). The Cys which provided amino for the further connection with C-dots attached to the surface of AuNPs by the Au-S bond. Approximately 5 mL AuNPs-Cys (0.05 $mg \cdot mL^{-1}$) was added dropwise to 5 mL C-dots solutions (0.2 $mg \cdot mL^{-1}$) which had been activated with EDC (0.01 M) and NHS (0.005 M) for 1 h. Next, the mixture was ultrasonically dispersed to obtain the C-Dots-AuNPs-Cys suspension. The obtained suspension was stored at 4 °C until further use.,

1.4 Cell culture. The HeLa cells, A549 cells, HUVEC cells and MDA-MB-231 cells were cultured in a Dulbecco's modified eagle medium (DMEM, Gibco, Grand Island, NY) supplemented with 10% fetal calf serum (FCS, Sigma), penicillin (100 $\mu g \cdot mL^{-1}$) and streptomycin (100 $\mu g \cdot mL^{-1}$) at 37 °C in a humidified atmosphere of 5% CO_2. The cells in the logarithmic growth phase were collected and separated from the medium through centrifugation at 1000 rpm for 5 min, and washed thrice with sterile PBS (pH 7.4). The collected sediments were then resuspended in physiological PBS to obtain the cell suspension of the appropriate concentration. The cells used in this work were primary culture cells. The cell number was determined using a blood counting chamber.

1.5 Fabrication of the biosensor. Briefly, the ITO electrode was cleaned via sonication by acetone, NaOH (1 M) in ethanol/water (1:1, v/v), and ultrapure water in series. After the

ITO electrode was dried, 20 μL C-dots-AuNPs-Cys suspension (0.06 $mg \cdot mL^{-1}$) was dropped onto the ITO electrode and then dried in a desiccator. The modified electrode was then rinsed with 100 μL PBS (pH 7.4, 0.01 M) and allowed to dry at room temperature. Next, 10 μL CS acetic acid solution (0.2% w/v) was dropped onto the electrode to provide the amino for further immobilization. FA (10 mg), EDC (20 mg) and NHS (10 mg) were mixed with 2 mL Tris-HCl buffer saline for 1 h to activate the carboxylate group. The modified electrode was stored in FA solution at 4 °C overnight to link the FA via an amide bond. After rinsing with PBS (pH 7.4, 0.01 M), the ITO/C-dots-AuNPs-Cys/CS/FA electrode was immersed into BSA solution (1% w/v) for 1 h at 37 °C to block the nonspecific binding sites. After carefully rinsing with 0.1 M PBS, the PEC cytosensor was obtained.

1.6 Cell Capture and measurement procedure. HeLa cells were chosen as a model, upon which the FR were over-expressed. The FA molecules immobilized on the electrode had a high affinity for the FR on the surface of the HeLa cell. Approximately 20 μL HeLa cell suspension at a certain concentration was dropped onto the PEC cytosensor interface and incubated at 37 °C for 1 h. After carefully rinsing with PBS, the cytosensor was inserted into the Tris-HCl buffered saline (0.1 M, pH 7.4) solution containing AA (0.05 M) to record the PEC response at an applied potential of -0.15 V under 405 nm irradiation. Different electrodes were used for continuous incubation of HeLa cells from low concentration to high value. The PEC detection system did not require deaeration with nitrogen.

1.7 MTT Assay. The cytotoxicity of the C-dots-AuNPs-Cys conjugates was analyzed by a MTT assay. The HeLa cell suspension was seeded in 96-well plates. Various concentrations of the C-dots-AuNPs-Cys conjugates were added to the experimental group cells and cultured for 24 h. MTT (0.2 mg/mL) was then added to each well and incubated for 4 h. The

supernatant was removed and the formazan crystals were dissolved in DMSO. The cell viability was assessed by measuring the absorbance at 550 nm using a microplate reader.

2. Characterization

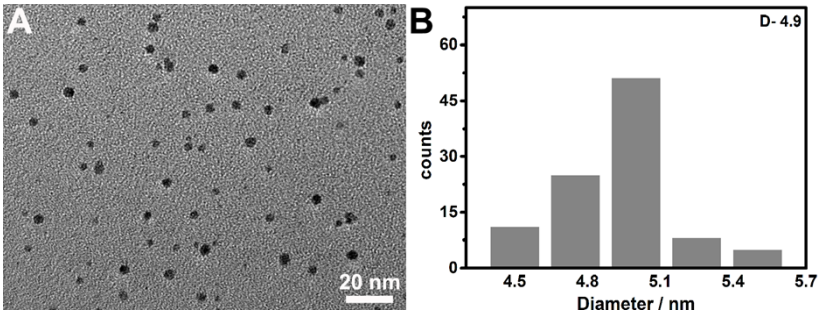

Fig. S1. HRTEM image of (A) AuNPs-Cys and (B) size distribution of AuNPs-Cys.

As show in Fig. S1-A, the distribution of the spherical AuNPs-Cys nanoparticles was even. The size of the AuNPs-Cys nanoparticles was estimated to be 4.9 nm (Fig. S1-B).

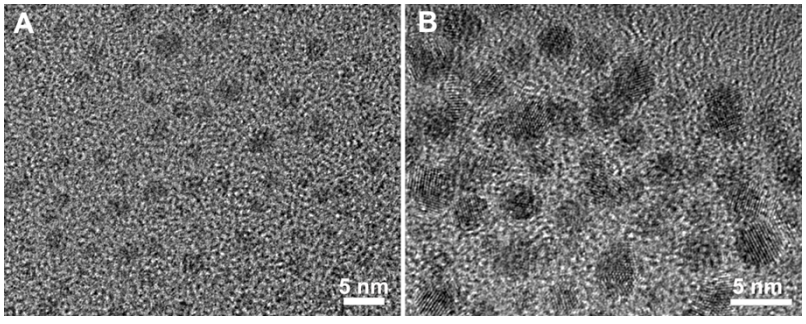

Fig. S2. HRTEM images of (A) C-dots and (B) C-dots-AuNPs-Cys.

As show in Fig. S2-A of the Supporting Information, the profile of the C-dots is spherical and their distribution is rather even. In addition, the average size of the C-dots is estimated to be 3 nm, which is consistent with previous research.[S3] When conjugating the C-dots with the AuNPs-Cys by amidation reaction, the C-dots came in close contact with the AuNPs-Cys, and the formed C-dots-AuNPs-Cys conjugates dispersed well, as shown in Fig. S2-B of the Supporting Information. This outcome is beneficial for photoinduced electron transfer

between the C-dots and AuNPs-Cys[S4] and is advantageous for fabricating a sensitive PEC cytosensor based on C-dots-AuNPs-Cys conjugates.

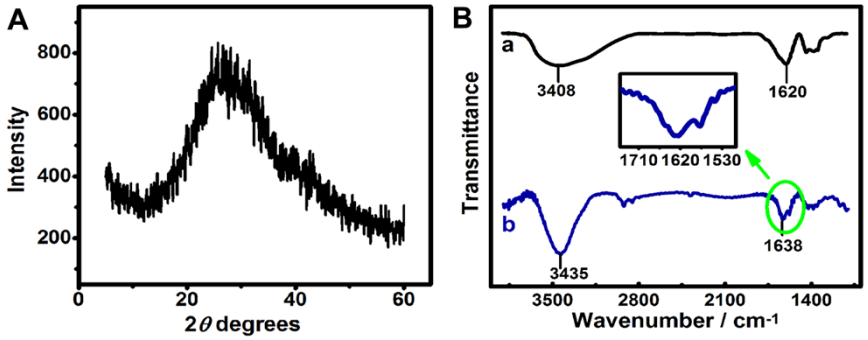

Fig. S3. (A) XRD pattern of C-dots. (B) FTIR spectra of C-dots (a) and C-dots-AuNPs-Cys (b).

The XRD measurement was utilized to verify the formation and evaluate the crystallinity of the C-dots (Fig. S3-A). The broad peak at 25.2° attested the successful synthesis of the C-dots, which exhibited an amorphous morphology.[S5] The formation of the C-dots-AuNPs-Cys conjugates is evidenced by the FTIR spectra (Fig. S3-B). The FTIR spectrum of the C-dots shows a broad band at 3408 cm^{-1} corresponding to the stretching vibrations of the O–H bond and a peak at 1620 cm^{-1} assigned to the stretching vibrations of the C=O bond (curve a), indicating the existence of carboxyl groups. The carboxyl groups are hydrophilic groups on the C-dots that improve the hydrophilicity of the C-dots. After conjugating the C-dots with AuNPs-Cys, the specific vibrations of the amide groups, amide I (1631 cm^{-1}) and amide II (1570 cm^{-1}), were observed in the FTIR spectrum of the C-dots-AuNPs-Cys (curve b), suggesting that the C-dots were linked to the AuNPs-Cys by the amidation reaction.[S6] Moreover, a broad band at 3435 cm^{-1} representing the stretching vibrations of the O–H bond was also observed, implying the existence of hydrophilic hydroxyl groups in the C-dots-AuNPs-Cys conjugates. The good hydrophilicity of the C-dots-AuNPs-Cys conjugates is

favorable for immobilizing cells on an electrode to construct a PEC cytosensor.

3. PEC responses and cell viability investigation

The cytotoxicity of the C-dots-AuNPs-Cys conjugates was studied using a 3-(4,5-dimethylthiazol-2-yl)-2,5-diphenyltetrazolium bromide (MTT) assay. The cell viability after incubating with the C-dots-AuNPs-Cys conjugates for 24 h is displayed in Fig. S4-B. The cell viability was 93.7% at a concentration of 60 ppm (the concentration of C-dots-AuNPs-Cys conjugates adopted in this assay), indicating that the PEC cytosensing substrate was hypotoxic and possessed a satisfactory biocompatibility that was superior to that of cadmium-containing quantum dots.[S7]

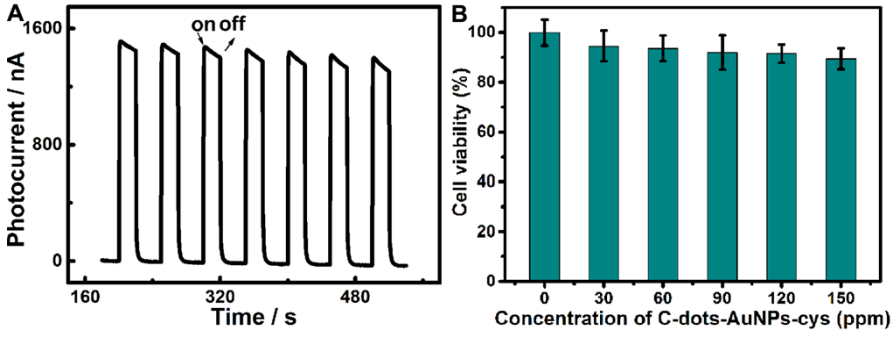

Fig. S4. (A) PEC responses of the C-dots-AuNPs-Cys modified ITO electrode at an applied potential of -0.15 V under 405 nm irradiation. (B) Cytotoxicity effect of C-dots-AuNPs-Cys on HeLa cells.

4. Optimization of the detection conditions

The incubation time was a relevant parameter for the capture of HeLa cells by FA on the C-dots-AuNPs-Cys/CS/FA/BSA modified ITO electrode. 20 μL HeLa cell suspension (1×10^5 cell·mL^{-1}) was dropped onto the modified electrode and incubated at 37 °C for 0.5, 1 and 1.5 h. The C-dots-AuNPs-Cys/CS/FA modified film showed excellent cell-capture

ability, as revealed by inverted fluorescence microscopy after staining with AO (Fig. S5). The FA molecules immobilized on the electrode had a high affinity for the FR on the surface of the HeLa cells. The amount of HeLa cells captured by the PEC cytosensor increased from 0.5 to 1 h and then leveled off from 1 to 1.5 h, indicating that the reaction equilibrium was reached and that the formation of FA-FR on the HeLa cells had reached saturation. Consequently, 1 h was selected as the optimal incubation time for PEC cytosensing.

The excitation wavelength was a significant factor influencing the PEC response (Fig. S6-A). At an applied potential of -0.15 V, the photocurrent slowly decreased as the wavelength increased from 385 nm to 405 nm and then markedly decreased as the wavelength increased further from 405 nm to 470 nm. The photocurrent at 405 nm and 430 nm was 85.6% and 59.2% of that at 385 nm, respectively. The photocurrent at 405 nm showed sufficient sensitivity for PEC detection. Moreover, a visible light excitation source was superior to ultraviolet light excitation source, which was favorable for the monitoring of biological systems and consumed less energy. Considering these two points, 405 nm was selected as the excitation wavelength for the PEC cytosensing.

The applied potential played a crucial role in the generation of the photocurrent (Fig. S6-B). Under 405 nm irradiation, the photocurrent decreased slightly from -0.25 V to -0.15 V and then deceased sharply from -0.15 V to -0.1 V. The photocurrent at -0.15 V and -0.1 V was 81.8% and 41.1% of that at -0.25 V, respectively. The photocurrent at -0.1 V was not sensitive enough for PEC measurement. Furthermore, the low applied potential was beneficial for the elimination of interference from other species coexisting in the cell suspension. Considering these findings, -0.15 V was chosen as the optimal applied potential for PEC cytosensing.

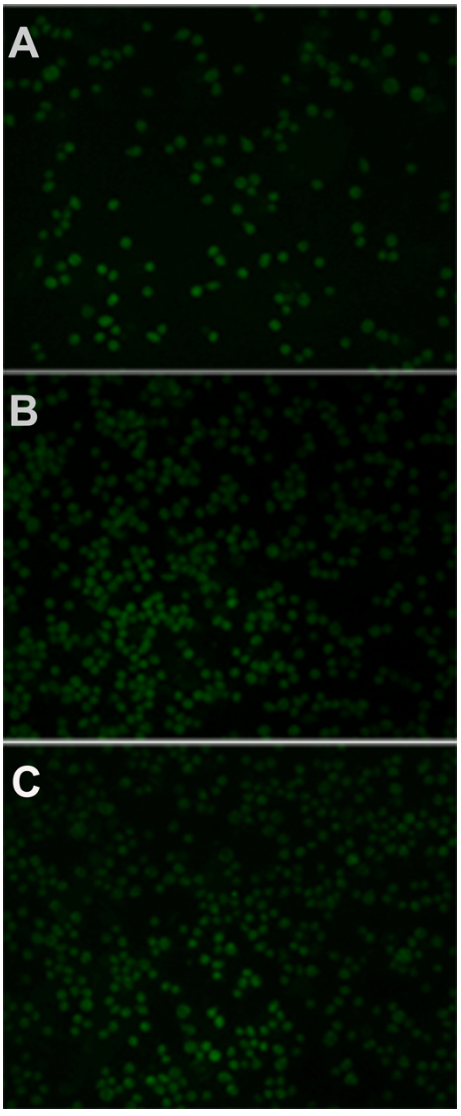

Fig. S5. Images of ITO/C-dots-AuNPs-Cys/CS/FA/BSA incubating with AO-stained HeLa cells at (A) 0.5 h, (B) 1 h and (C) 1.5 h.

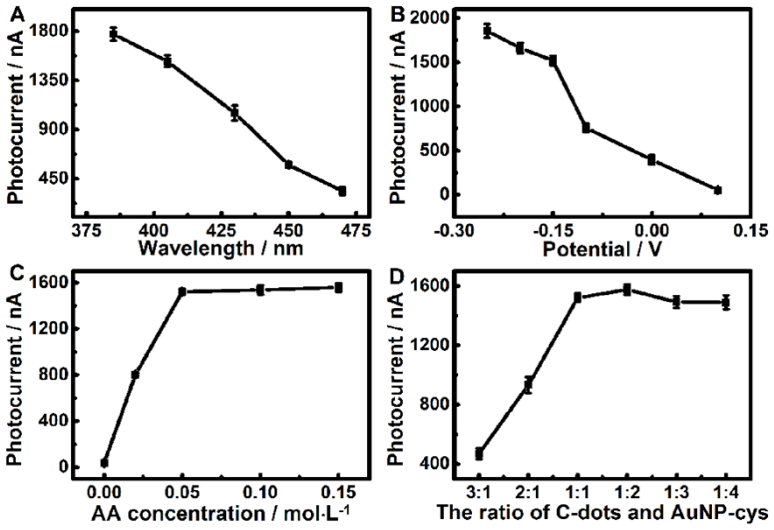

Fig. S6. Effects of (A) excitation wavelength, (B) applied potential, (C) AA concentration and (D) the ratio of C-dots and AuNPs-Cys on the photocurrent responses of the C-dots-AuNPs-Cys modified ITO electrode.

The concentration of AA, the electron donor, was another key factor in obtaining a stable and intense photocurrent (Fig. S6-C). When the concentration of AA was increased from 0 to 0.05 M, the photocurrent intensity increased markedly, plateauing at 0.05 M. Concentrations greater than 0.05 M did not improve the PEC response. Therefore, 0.05 M was the optimal concentration for the PEC measurement.

Furthermore, the ratio of the C-dots and the AuNPs-Cys was studied to obtain an optimal PEC response for cytosensing (Fig. S6-D). The photocurrent increased rapidly as the C-dots:AuNPs-Cys ratio decreased from 3:1 to 1:1 and then leveled off as it was decreased further from 1:1 to 1:4. Thus, a C-dots:AuNPs-Cys ratio of 1:1 was optimal for PEC determination.

Table S1. The performance comparison of the proposed strategy with the previous reported researches for the detection of cell.

detection methods	cell line	linear range (cell·mL^{-1})	detection limit (cell·mL^{-1})	reference
Colorimetry	HeLa	1×10^3-3×10^5	1000	S8
PEC (CdS QDs)	SMMC-7721	5×10^3-1×10^7	5.0×10^3	S9
ICP-MS	Jurkat T	3×10^2-3×10^4	84	S10
EIS	HeLa	1×10^3-1×10^6	794	S11
Magnet-QCM	Leukemia	1×10^4-1.5×10^5	8000	S12
PEC	HeLa	1×10^2-5×10^6	15	this work

5. The selectivity of the cytosensor

To evaluate the selectivity of the proposed method, HUVEC cells (FR-), A549 cells (FR-) and MDA-MB-231 cells (FR+) were investigated through the photocurrent change ($\Delta I = I_0 - I$, where I_0 is the photocurrent of $C_{cell} = 1\times 10^4$ cell·mL^{-1} and I is the photocurrent of $C_{cell} = 0$) under the same conditions. As shown in Fig. S7, the PEC response of HUVEC cells (FR-), A549 cells (FR-) and MDA-MB-231 cells (FR+) were 7.6%, 9.6% and 23.2% of that of HeLa cells, respectively. The results showed that only tumor cells overexpressed with FR could induce the obvious PEC response, indicating the designed PEC assay method had good selectivity.

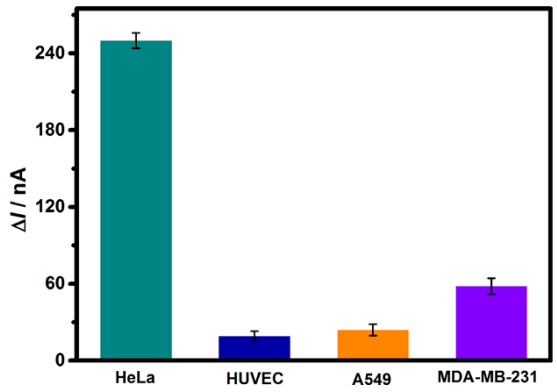

Fig. S7. PEC response of the cytosensor to HeLa cells, HUVEC cells, A549 cells and MDA-MB-231 cells.

References

S1 J. T. Li, S. K. Cushing, P. Zheng, F. K. Meng, D. Chu and N. Q. Wu, *Nat. Commun.*, 2013, **4**, 2651.

S2 A. S. Ramirez-Segovia, J. A. Banda-Aleman, S. Gutierrez-Granados, A. Rodriguez, F. J. Rodriguez, L. A. Godinez, E. Bustos and J. Manriquez, *Anal. Chim. Acta*, 2014, **812**, 18.

S3 S. K. Cushing, J. T. Li, F. K. Meng, T. R. Senty, S. Suri, M. J. Zhi, M. Li, A. D. Bristow and N. Q. Wu, *J. Am. Chem. Soc.*, 2012, **134**, 15033.

S4 L. Sheeney-Haj-Ichia, S. Pogorelova, Y. Gofer and I. Willner, *Adv. Funct. Mater.*, 2004, **14**, 416.

S5 A. Prasannan and T. Imae, *Ind. Eng. Chem. Res.*, 2013, **52**, 15673.

S6 J. Zong, X. L.Yang, A. Trinchi, S. Hardin, I. Cole, Y. H. Zhu, C. Z. Li, T. Muster and G. Wei, *Nanoscale*, 2013, **5**, 11200.

S7 D. W. Huang, C. G. Niu, M. Ruan, X. Y. Wang, G. M. Zeng and C. H. Deng,

Environ. Sci. Technol., 2013, **47**, 4392.

S8 Y. J. Song, Y. Chen, L. Y. Feng, J. S. Ren and X. G. Qu, *Chem. Commun.*, 2011, **47**, 4436.

S9 Z. Qian, H. J. Bai, G. L.Wang, J. J. Xu and H. Y. Chen, *Biosens. Bioelectron.*, 2010, **25**, 2045.

S10 Y. Zhang, B. B. Chen, M. He, B. Yang, J. Zhang and B. Hu, *Anal. Chem.*, 2014, **86**, 8082.

S11 L. Y. Feng, Y. Chen, J. S. Ren and X. G. Qu, *Biomaterials*, 2011, **32**, 2930.

S12 Y. L. Pan, M. L. Guo, Z. Nie, Y. Huang, C. F. Pan, K. Zeng, Y. Zhang and S. Z. Yao, *Biosens. Bioelectron.*, 2010, **25**, 1609.